

A New Method for Measuring Strain Using Slice Following with Inversion Recovery (SFIR)

T. A. Yousef^{1,2}, K. Z. Abd-Elmoniem¹, and N. F. Osman^{1,2}

¹ECE Dept., Johns Hopkins University, Baltimore, MD, United States, ²Department of Radiology, Johns Hopkins University, Baltimore, MD, United States

Introduction: MRI is a unique modality in imaging the motion of moving tissues including that of the heart. Tagging and phase contrast techniques have been used to noninvasively measure the myocardium motion. In this work, a new technique is proposed to measure the through-plane strain based on the changes in slice profile due to tissue deformation.

Theory: The new method consists of three steps:

Step 1) Slice Following Imaging: In slice following imaging [1], a thin slice is inverted with a slice selective 180° inversion pulse before the deformation, while a thicker slice—thick enough to enclose the initially inverted slice—is selected for imaging. Another acquisition does not invert a slice and just image the thicker one. The two acquisitions are then subtracted to yield an image of the tissue of inverted slice (Fig. 1). In case any deformation occurs to the inverted slice, the slice thickness changes accordingly and accompanied by changes in the z frequency domain. In case of a rectangular slice profile, changes in the slice thickness will result in changing the width and magnitude of the sinc profile in the frequency domain.

Step 2) Tuning in z-direction: Assuming the image plane is the x-y plane, the Fourier transform $S(\omega_z)$ of the slice profile $s(z)$

is real, symmetric and centered around ($k_z = 0$). In order to capture any information at a specific point on this profile (other than $k_z = 0$), a gradient field $G_z(\tau)$ is applied in the z-direction during the refocusing lobe. This can be seen as a phase encoding in the z-direction with the value $k_z = \gamma \int G_z(\tau) d\tau$. The resulting image is the integral, in z-direction, of the longitudinal magnetization multiplied by the z-encoding phase factor over the slice profile $s(z)$. So, the intensity of an arbitrary pixel located at (x,y,t) can be given as $I(x, y, t, \omega_d) = \int \rho(x, y, t) s(z) e^{-j\omega_d z} dz = \rho(x, y, t) S(\omega_d)$, where $\rho(\cdot)$ represents the signal intensity of the voxel due to the tissue properties such as proton density, T₁ or T₂ parameters. We call ω_d in (1) the tuning frequency of the acquired image.

Step 3) Imaging Technique: In order to capture the tissue deformation, a complete knowledge about the slice profile in frequency domain is needed. For a rectangular slice profile ($s(z) = \text{rect}(z/B)$ and $S(\omega_z) = \text{sinc}(B\omega_z)$), two samples at two different z-frequency are sufficient to fully describe the sinc function—which can be done by acquiring two images with the corresponding two tunings.

Step 4) Strain Computations: For a voxel with initial slice thickness B_0 , Two intensities are acquired at two different

tuning frequencies, I_0 at $\omega_d = 0$ and I_1 at $\omega_d = \omega_1$ then the new slice thickness at time t (B_t) can be estimated as follows:

$$B_t = \frac{\text{sinc}^{-1}(I_1 / I_0)}{\omega_1}, \quad (2)$$

Then the local strain (ϵ_t) can be estimated using: $\epsilon_t = (B_t / B_0) - 1$. (3).

Methods: First, to validate the theory, A phantom study was conducted using a clinical 3T MR whole-

body system (Gyrosan Intera; Philips Medical System, Best, The Netherlands). A cubic phantom of side length 4' was compressed with a balloon blown with air and purged in constant time intervals, in the normal direction to the image plane. R-wave is simulated exactly before when the balloon start to be blown. The balloon diameter was 1.5 inches during its maximum blowing and was positioned in one corner of the phantom to allow compression in this corner and stretching in the opposite corner. Two slice following image sets were acquired at two different tunings (0, 0.6). The two sets were used to calculate

the width of the sinc profile and hence estimate the strain in each voxel using the proposed algorithm. Next, a normal volunteer was imaged. Two short axis-slice following image sets were acquired with the same tuning as the phantom study, and then the longitudinal strain maps were estimated. In both the two studies, the strain

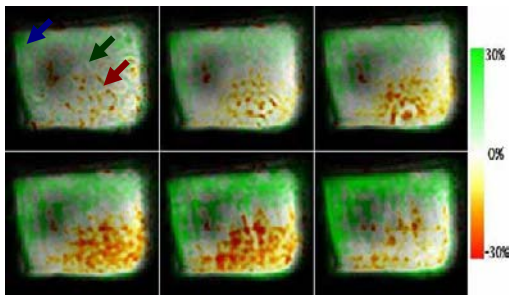


Fig 3: Cine time frames of the constructed function images for the phantom. Time frames (from top-left) are at 91, 251, 411, 571, 731, 891msec starting exactly when the balloon start to be blown. The annotated points in the first frame refer to the points that have been used for strain curves in fig. 2.

the width of the sinc profile and hence estimate the strain in each voxel using the proposed algorithm. Next, a normal volunteer was imaged. Two short axis-slice following image sets were acquired with the same tuning as the phantom study, and then the longitudinal strain maps were estimated. In both the two studies, the strain

Results & Discussion: Fig. 2 shows the strain curves for three different areas of the phantom (annotated in first frame of Fig. 3).

Fig. 3 shows the phantom function images in time frames spanning the whole compression cycle (corresponding to frames #2, 4, 6, 8, 10, 12 in fig. 2). The maximum compression appears at frame #10 while the last two frames appears are taken during the balloon purging. Fig.4 shows the strain curves for three pixels in the myocardium and a pixel in the static tissue. Fig. 5 shows the function images of the acquired short axis (corresponding to frames #1, 3, 5, 7, 9, 11, 13). Note the behavior of the different tissue types (either uniform dark spot in the upper left corner of the phantom-appears biased toward compression- or the fat regions around the myocardium –appears biased toward stretching-), it's clear that the slice thickness for these tissues are different than their surrounding. However, more analysis is required in order fully understand this effect.

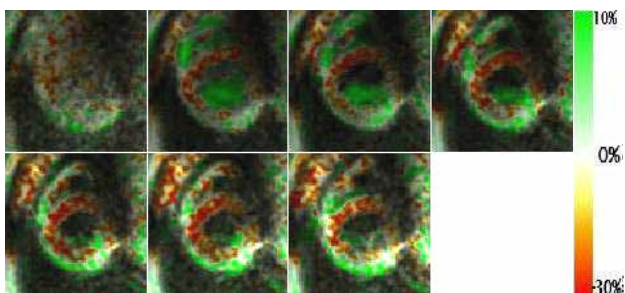


Fig 5: Cine time frames of the constructed function images for the cardiac short axis with ROI around the myocardium. Time frames (from top-left) are at 41, 101, 161, 221, 281, 341, 401msec starting exactly after the R-wave.

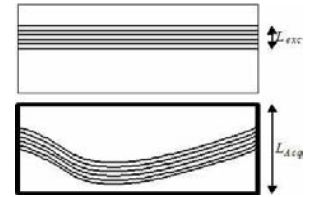


Fig 1: Slice following concept. Thin slice (L_{inv}) is inverted and a thicker slice (L_{Acq}) is imaged twice, one after the inversion and one without it. The, the two images are subtracted.

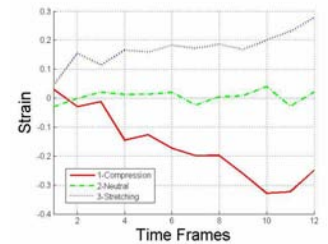


Fig 2: Strain curves for three points from different areas of deformation in the phantom (The points' areas are shown in the first time frame of fig. 3)

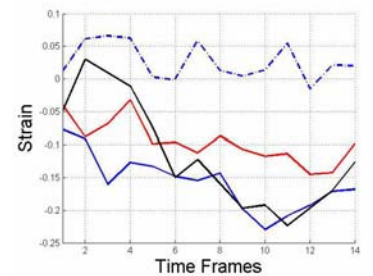


Fig 4: Strain curves for 3 points in the myocardium and one point in the static tissue outside the myocardium.

Conclusion: New technique is proposed for estimating the through plane tissue deformation from the normal slice following images. No special patterns or phase encoding are needed. Extra information (like the in-plane motion) can be encoded in the image plane without affecting the strain measurements.

References: [1] M. Stuber et al, "Slice Following in Cardiac Imaging with Optimized RF Pulse Angles," Proc ISMRM, p. 418.